Journal of Materials Chemistry C

Accepted Manuscript

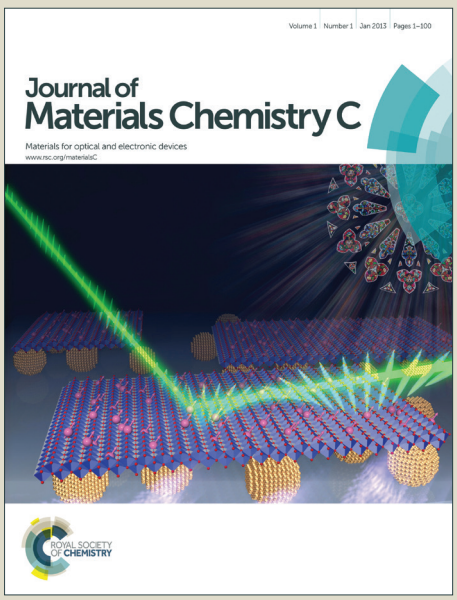

ROYAL SOCIETY OF CHEMISTRY

www.rsc.org/materialsC

Cite this: DOI: 10.1039/c0xx00000x

www.rsc.org/materials

PAPER

M^{3+}[amaranth red]$^{3-}$ (M = La, Gd): A Novel Sulfonate-based Inorganic-Organic Hybrid Nanomaterial for Multimodal Imaging

Marieke Poß,[a] Joanna Napp,[b] Oliver Niehaus,[c] Rainer Pöttgen,[c] Frauke Alves,[b] and Claus Feldmann[a]*

Received (in XXX, XXX) Xth XXXXXXXXX 2012, Accepted Xth XXXXXXXXX 20XX

DOI: 10.1039/b000000x

Lanthanum and Gadolinium amaranth-red hybrid nanoparticles consist of an inorganic cation M^{3+} (M = La, Gd) and the fluorescent organic dye anion [AMA]$^{3-}$ (AMA: amaranth red, $C_{20}H_{11}N_2O_{10}S_3$) that is systematically named (4E)-3-oxo-4-[(4-sulfonatonaphth-1-yl)hydrazinyliden]naphthalin-2,7-disulfonate (as well named E123, C.I. 16185, Acid Red 27, C-Red 46, Echtrot D, or Food Red 9). M^{3+}[AMA]$^{3-}$ (M = La, Gd) nanoparticles are prepared via aqueous synthesis as highly stable colloidal suspensions with a mean particle diameter of 47 nm. The chemical composition is validated by infrared spectroscopy (FT-IR), energy-dispersive X-ray analysis (EDX), thermogravimetry (TG) and elemental analysis (EA). M^{3+}[AMA]$^{3-}$ (M = La, Gd) shows intense red emission (λ_{max} = 700 nm) upon excitation at 400-650 nm. Even after 15 hours of UV irradiation (310 nm), the nanoparticles do not show any significant photobleaching. Based on its red fluorescence and its Gd^{3+}-based magnetism, especially, Gd^{3+}[AMA]$^{3-}$ nanoparticles can be interesting as a multimodal contrast agent for biomedical applications or as a magneto-optical marker in polymers. This holds even more in view of biocompatibility, high dye load (79 wt-%), excellent photostability, and water-based synthesis of the M^{3+}[AMA]$^{3-}$ (M = La, Gd) inorganic-organic hybrid nanoparticles.

1. Introduction

Organic fluorescent dye molecules are widely used for marking, signalling and detection, for instance, in/on polymers, paper (e.g. bank notes) as well as for optical imaging in biology and medicine.[1,2] To the latter concern, a manifold of organic fluorescent dyes, stains and labelled proteins showing fluorescence from the blue to the infrared spectral range were developed since the beginning of fluorescence microscopy in the early 20th century to analyze all kinds of biological probes.[2] Essential requirements for such fluorescent dyes include high emission intensity, high photostability as well as chemical resistance against the conditions of the relevant environment.[3]

Many conventional fluorescent dyes do not meet one or more of the above demands. Especially, photobleaching is a major challenge for many organic fluorescent dyes and an issue for all kinds of application, including fluorescence microscopy.[4,5] As an alternative, semiconductor-type quantum dots (Q-dots such as CdSe) are well-known for their unique brightness and excellent photostability.[6] As Q-dots have disadvantages like toxic metals as constituents, advanced core-shell structures, high demands on size control and crystallinity, alternative concepts are eligible for the use of standard, less harmful fluorescent dyes, but at significantly increased photostability.[7]

In addition to fluorescent dye molecules in solution, fluorescent organic dyes – including various derivatives of rhodamin, cyanin, squarain, boron-dipyrromethene, porphyrin or phtalocyanin[8] – were encapsulated in inorganic matrices (e.g., silica, $CaPO_4$),[9] organic polymers (e.g., polyglycolic acid/PGA, polylactic acid/PLA, poly(lactic-*co*-glycolic acid/PLGA, polycaprolactone/PCL, chitosan),[10] or liposomes.[11] For some of these composite materials, a certain increase of the photostability was observed in comparison to the dissolved fluorescent dye molecule. Nevertheless, considerable photobleaching – to the best of our knowledge – was observed after certain period of continuous illumination.[7-13]

In this work, we present the novel sulfonate-based inorganic-organic hybrid nanoparticles with a composition M^{3+}[AMA]$^{3-}$ (M = La, Gd) (Figure 1). Herein, the organic dye anion [AMA]$^{3-}$ (AMA: amaranth red, $C_{20}H_{11}N_2O_{10}S_3$, systematically named (4E)-3-oxo-4-[(4-sulfonatonaphth-1-yl)hydrazinyliden]aphthalin-2,7-disulfonate) shows characteristic red emission at λ_{max} = 700 nm. Amaranth red (also known as E123, C.I. 16185, Acid Red 27, C-Red 46, Echtrot D, or Food Red 9) is widely used, for instance, in food industry.[14] Thus, it can be considered as a less harmful fluorescent dye. The concept of sulfonate-based inorganic-organic hybrid nanoparticles is first presented with M^{3+}[AMA]$^{3-}$ (M = La, Gd) and comprises several advantages: (*i*) Water-based synthesis; (*ii*) Less-harmful nanoparticles being available as colloidally stable aqueous suspension right after synthesis; (*iii*) Enormous dye load (79 wt-%); (*iv*) High photostability even under UV illumination; (*v*) Option for

[a]*Institut für Anorganische Chemie, Karlsruhe Institute of Technology (KIT), Engesserstrasse 15, 76131 Karlsruhe, Germany; Fax: +49-721-60844892; Tel: +49-721-60842855; E-mail: claus.feldmann@kit.edu.*

[b]*Max Planck Institute of Experimental Medicine, Robert-Koch-Str. 40, 37075 Göttingen, Germany.*

[c]*Institut für Anorganische und Analytische Chemie, University of Münster, Corrensstraße 30, 48149 Münster, Germany.*

multimodal detection and marking based on the red fluorescence of $[AMA]^{3-}$ and the intrinsic paramagnetism related to Gd^{3+}.

2. Experimental Section

2.1. Synthesis

Synthesis of $M^{3+}[AMA]^{3-}$ ($M = La^{3+}$, Gd^{3+}; AMA = amaranth red) nanoparticles: $M^{3+}[AMA]^{3-}$ hybrid nanoparticles were synthesized via the following procedure: First, $Na_3[AMA]$ (120 mg, 0.2 mmol, AMA = $C_{20}H_{11}N_2O_{10}S_3$, 85-95%, Sigma, Germany) was dissolved in water (90 mL). This solution was heated to 55° C and stirred vigorously. Thereafter, an aqueous solution (0.5 mL) containing $LaCl_3{\times}7H_2O$ (74 mg, 0.2mmol, >98.5%, Fluka, Germany) or $GdCl_3{\times}6H_2O$ (74 mg, 0.2mmol, 99%, Aldrich, Germany) were injected. After 2 min of intense stirring, the nanoparticles were separated via centrifugation (25,000 RPM, 15 min). To remove all remaining salts, the dark red nanoparticles were resuspended in and centrifuged from H_2O three times. The resulting nanoparticles can be resuspended in H_2O, HEPES buffer or Dextran solution via mechanic stirring or ultrasonification in order to get stable suspensions with a weight content of 1 mg/mL.

2.2 Analytical tools

Dynamic light scattering (DLS) was used to determine the hydrodynamic diameter of the nanoparticles and their size distribution in suspension. Studies were conducted in polystyrene cuvettes applying a Nanosizer ZS (Malvern Instruments, United Kingdom).

Zeta potential measurements were conducted using an automatic titrator MPT-2 attached to the Nanosizer ZS (Malvern Instruments, United Kingdom). For a typical measurement, 1 mL of a suspension containing 5 mg/mL of $M^{3+}[AMA]^{3-}$ nanoparticles was diluted with 9 mL of demineralized water. Titration was performed using 0.1M HCl and 0.1M NaOH.

Scanning electron microscopy (SEM) was carried out with a Zeiss Supra 40 VP (Zeiss, Germany), equipped with a field emission gun (acceleration voltage 1 kV, working distance 3 mm). Samples were prepared by placing a droplet of a diluted aqueous suspension of the nanoparticles on a silica wafer that was left for drying overnight.

Energy-dispersive X-ray (EDX) analysis was performed with an Ametek EDAX (Ametek, U.S.), device mounted on the above described Zeiss SEM Supra 40 VP. For this purpose, the nanoparticles were pressed to dense pellets in order to guarantee for a smooth surface and a quasi-infinite layer thickness. These pellets were fixed with conductive carbon pads on aluminium sample holders. EDX was only used to validate the presence of lanthanum, gadolinium and sulphur in $[M]^{3+}[AMA]^{3-}$ hybrid nanoparticles. A quantification of La/Gd/S or determination of the lighter elements C/N/O/H was not performed via this method due to limited significance.

X-ray powder diffraction (XRD) measurements were conducted with a Stadi-P diffractometer (Stoe, Germany) with Ge-monochromatized Cu-Kα radiation. The dried samples were fixed between Scotch tape and acetate paper and measured between -69 ° and +69 °of two-theta.

Fourier-transformed infrared (FTIR) spectra were recorded with a Bruker Vertex 70 FT-IR spectrometer (Bruker, Germany) in the range 4000–370 cm^{-1} with a resolution of 4 cm^{-1}. To this concern, 1 mg of dried sample was pestled with 300 mg of KBr and pressed to a pellet.

Differential thermal analysis/thermogravimetry (DTA/TG) was performed with a STA409C device (Netzsch, Germany). The measurements were performed in air. The vacuum dried samples (20 mg in corundum crucibles) were heated to 1000 °C with a rate of 1 K/min.

Elemental analysis (C/H/N/S analysis) was performed via thermal combustion with an Elementar Vario Microcube device (Elementar, Germany) at a temperature of about 1100 °C.

Photoluminescence (PL) and photobleaching were recorded with a Horiba Jobin Yvon Spex Fluorolog 3 (Horiba Jobin Yvon, France) equipped with a 450 W Xe-lamp and double grating excitation and emission monochromator.

Magnetic measurements of $Gd^{3+}[AMA]^{3-}$ were carried out on a Quantum Design Physical Property Measurement System (Quantum Design, U.S.) using the vibrating sample magnetometer (VSM) option. For the measurement, 11 mg of the powdered samples were packed in polypropylene capsules and attached to the sample holder rod. Magnetic investigations were performed in the temperature range of 3 to 350 K with magnetic flux densities up to 80 kOe.

Polymers with $La^{3+}[AMA]^{3-}$ *nanoparticles:* $La^{3+}[AMA]^{3-}$ hybrid nanoparticles were embedded in polyester matrices following the recipe given by *Blume et al.*.[15] Briefly, 0.2 mg, 1.0 mg or 5.0 mg of $La^{3+}[AMA]^{3-}$ hybrid nanoparticles were redispersed in 5 mL ethylene glycol. Under vigorous stirring, thereafter, 11.3 g of citric acid were added and heated until the citric acid was dissolved completely. The resulting highly viscous polymer was poured into a culture dish and cooled to room temperature. After synthesis, a viscid, soft and water insoluble transparent resin was received, containing 0.2-5.0 mg of $La^{3+}[AMA]^{3-}$ per 1 mL of ethylene glycol.

Cell culture: MH-S mouse alveolar macrophages[16] were propagated in RPMI 1640 medium supplemented with 0.05 mM/L β-mercaptoethanol and 10% FCS. The cells were cultivated under standard cell culture conditions at 37 °C in a humidified atmosphere under 5% CO_2.

Incubation with fluorescent nanoparticles: MH-S cells were seeded on cover glasses placed in 24-well plates (50.000 cells per well). After 48 h, the medium was removed and the macrophages were supplemented with 1 mL medium containing 50 µg/mL of $Gd^{3+}[AMA]^{3-}$ hybrid nanoparticles. Macrophages were co-incubated with the nanoparticles either for 5 h or 24 h at 37 °C or at 4 °C as a control, the condition when the metabolism was slowed down and the internalization was inhibited. Afterwards, cells were washed with PBS, fixed with 4% paraformaldehyde in PBS for 10 min and washed with PBS again. Cells were mounted with *ProLong* Gold *Antifade* Reagent with *DAPI* (Invitrogen, U.S.) for counter stain of cell nuclei and analyzed by fluorescence microscopy.

Microscopy and image analysis: Fluorescence microscopy was performed using a Zeiss Axiovert 200 M inverted microscope (Carl Zeiss, Germany), equipped with a xenon lamp and a high sensitivity ORCA-AG digital camera (Hamamatsu,

Cite this: DOI: 10.1039/c0xx00000x

www.rsc.org/xxxxxx

PAPER

Japan). For $Gd^{3+}[AMA]^{3-}$ hybrid nanoparticles a 546/12 nm excitation filter and a 590 nm long pass emission filter was used. Image generation and processing were performed with the software AxioVision Rel.4.6 and ImageJ (available by ftp at *zippy.nimh.nih.gov* or at *http://rsb.info.nih.gov/nih-imageJ*; developed by Wayne Rasband (National Institutes of Health, U.S.), respectively.

Cell viability assay: 24 h prior to the experiment, MH-S cells were plated in 96-Well plates at a concentration of 5.000 cells per Well in 100 µL of medium. After 24 h the medium was replaced by a fresh one (100 µL/Well) containing increasing concentrations (0-200 µg/mL) of the $Gd^{3+}[AMA]^{3-}$ nanoparticles. The influence of the nanoparticles on proliferation and viability of the cells were quantified after 24 h and 48 h of treatment using CellTiter 96 AQueous One Solution Cell Proliferation Assay (Promega) according to the manufacturer's protocol by measuring the absorbance of the formazan dye (produced by viable cells; absorbance measured at 450 nm) using the Wallace 1420 Victor 2 Multilabel Counter (American Instrument Exchange). To obtain only signals derived from the formazan dye, the absorbance of the corresponding $Gd^{3+}[AMA]^{3-}$ solutions in cell culture medium was measured afterwards and subtracted from particular cell-measurements. The relative viability was calculated as a ratio between treated and untreated cells after subtraction of the absorbance of corresponding nanoparticle-medium solution. Experiment was performed in triplicate.

3. Results and discussion

3.1. Synthesis of $M^{3+}[AMA]^{3-}$ inorganic-organic hybrid nanoparticles (M = La, Gd; AMA = amaranth red)

The inorganic-organic hybrid nanomaterial $M^{3+}[AMA]^{3-}$ with M = La, Gd and AMA = amaranth red/$C_{20}H_{11}N_2O_{10}S_3$ – in correlation to the latin origin *"hybrid = crossbreed"* – combines two parts intermixed on the molecular level. Similar to simple sodium chloride – containing equimolar amounts of Na^+ cations and Cl^- anions – the sulfonate-based hybrid nanoparticles consist of equimolar amounts of La^{3+} or Gd^{3+} (as inorganic cation) and the organic fluorescent dye anion amaranth red $[AMA]^{3-}$ (Figure 1). Based on molar quantities of the fluorescent dye as the anion, naturally, the weight load of the fluorescent dye per nanoparticles is extraordinarily high, and reaches 79 wt-% for $La^{3+}[AMA]^{3-}$ and 77 wt-% for $Gd^{3+}[AMA]^{3-}$.

We have successfully presented such materials concept already for phosphate-based inorganic-organic hybrids such as $[ZrO]^{2+}[FMN]^{2-}$ (FMN = flavinmononucleotide) showing green emission.[17] However, the number of commercially available fluorescent dyes with a phosphate functionality is comparably limited. Moreover, phosphate-functionalized dyes for red and infrared emission are often extremely expensive (up to 300 € per 1 mg).[4] In contrast, almost all conventional fluorescent dyes are commercially available with a sulfonate functionality. Hence, sulfonate-based inorganic-organic hybrids can significantly broaden the scope in comparison to phosphate-based hybrid nanoparticles.

The synthesis of $M^{3+}[AMA]^{3-}$ (M = La, Gd), in concrete, is performed via uncomplex forced hydrolysis in water (Figure 1).[18] To this concern, an aqueous solution of $Na_3[AMA]$ was mixed with a second aqueous solution of $LaCl_3{\times}7H_2O$ or $GdCl_3{\times}6H_2O$. To obtain nanoparticles and colloidally stable suspensions, general aspects – following LaMer's model – for controlling particle nucleation and particle growth have to be considered.[19] Hence the solution of the rare-earth metal chloride was injected under vigorous stirring at slightly increased temperature (55 °C). Moreover, the dye anion was used with 10 mol-% excess in relation to the cation in order to guarantee for anion-terminated particle surfaces. Subsequent to synthesis, the nanoparticles were three times centrifuged and redispersed from/in water in order to remove all remaining salts and starting materials. Finally, the $M^{3+}[AMA]^{3-}$ nanoparticles can be easily suspended in solvents, such as diethylene glycol (DEG), ethanol, water or biological buffers like HEPES or aqueous dextran.

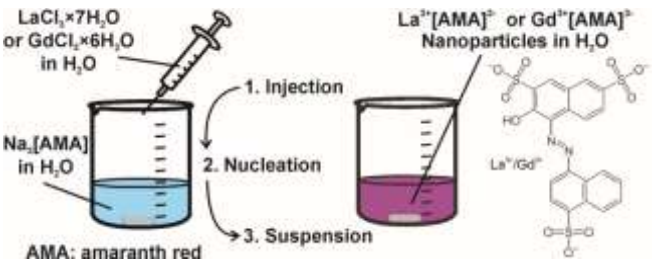

Fig. 1. Scheme illustrating the synthesis of the inorganic-organic hybrid nanoparticles $La^{3+}[AMA]^{3-}$ and $Gd^{3+}[AMA]^{3-}$ (AMA: amaranth red, $C_{10}H_{11}S_3N_2O_{10}$).

It is to be noted that the $M^{3+}[AMA]^{3-}$ nanoparticles are readily available as colloidally stable aqueous suspensions after synthesis. Neither advanced multistep synthesis, core-shell structures, nor specific demands regarding materials crystallinity or surface conditioning for dispersion in water have to addressed, which is a major difference to Q-dots,[6] and which facilitates the synthesis of sulfonate-based hybrid nanoparticles enormously. Based on such synthesis strategy, $M^{3+}[AMA]^{3-}$ (M = La,Gd) nanoparticles are also accessible in large quantities (10 g $M^{3+}[AMA]^{3-}$ nanoparticles made in 1 L of water) and concentrated suspensions (up to 10 mg/mL).

3.2 Particles size and chemical composition of $M^{3+}[AMA]^{3-}$ inorganic-organic hybrid nanoparticles

The particle diameter of the as-prepared $M^{3+}[AMA]^{3-}$ nanoparticles was validated by dynamic light scattering (DLS). To verify the primary particle diameter, first of all, diethylene glycol (DEG) was used as it is known for excellent stabilization of nanoparticles via surface coordination.[20] Here, a mean hydrodynamic diameter of 68(10) nm at narrow size distribution is observed (Figure 2a). In water – as a highly polar solvent – nanoparticles typically show larger hydrodynamic radii due to a

comparably extended rigid adsorption layer of solvent molecules that are fixed via hydrogen bonding as well as due to certain agglomeration. Thus, a mean hydrodynamic diameter of 105(30) nm is observed in H_2O (Figure 2a). Moreover, the particle diameter of powder samples was investigated via scanning electron microscopy (SEM). Here, overview images show uniform spherical particles with a mean diameter of 47(10) nm (Figure 2b). This value was calculated by statistical evaluation of 130 particles. The larger particle diameter obtained from DLS – as expected – reflects the hydrodynamic diameter and the presence of a rigid layer of adsorbed H_2O molecules on the particle surface.

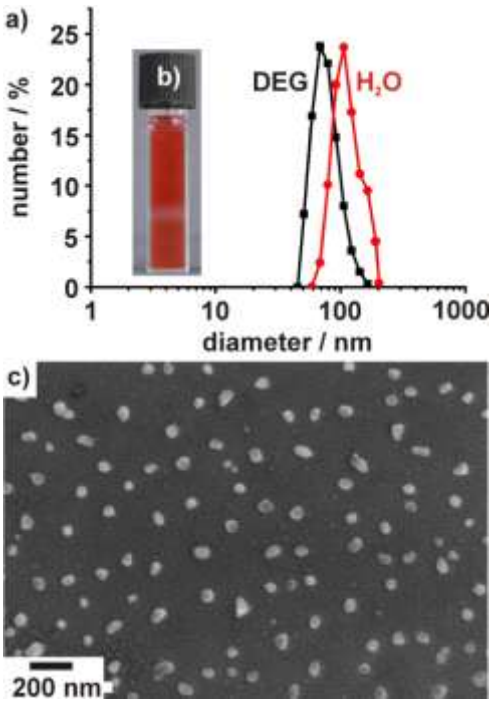

Fig. 2. Particle size and size distribution of $M^{3+}[AMA]^{3-}$ (M = La, Gd) hybrid nanoparticles: a) DLS analysis in diethylene glycol (DEG) and water; b) Cuvette with suspension in water (1 mg/mL); c) SEM image.

In addition, the Zeta potential of the inorganic-organic hybrid nanoparticles was determined in water and resulted in a value of –12.5 mV in the biologically most relevant pH range from pH 4 to pH 8 (Figure 3). Due to this negative surface charge and the resulting electrostatic stabilization, preparation of the nanoparticles via forced hydrolysis in water is possible. For biomedical application, furthermore, the as-prepared $M^{3+}[AMA]^{3-}$ nanoparticles can be coated by dextran to support membrane permeability and cell uptake.[21]

To prove the chemical composition of the inorganic-organic hybrid nanoparticles, different analytical methods were involved. First of all, proving the presence of the organic dye anion $[AMA]^{3-}$ and the inorganic cation La^{3+} or Gd^{3+} is most important. Here, Fourier-transform infrared spectroscopy (FT-IR) evidences the presence of the organic dye anion (Figure 4a). FT-IR spectra of the $M^{3+}[AMA]^{3-}$ nanoparticles show all characteristic vibrations of amaranth red, including ν (O-H): 3600-3000 cm^{-1}; ν (N=N): 1370 cm^{-1}, ν (C-N=N-C): 1230 cm^{-1}, ν (SO_3): 680-420 cm^{-1}.[22] For direct comparison, the FT-IR spectrum of the starting material $Na_3[AMA]$ is displayed as a reference (Figure 4a). Altogether, all relevant vibrations of the reference are detected for the nanoparticles as well. It is to be noted that a certain broadening of all vibrations of $M^{3+}[AMA]^{3-}$ is related to the non-crystallinity of the nanoparticles. Besides the presence of the amaranth-red anion, the presence of lanthanum or gadolinium and sulphur was qualitatively proven by energy dispersive X-ray analysis (EDX). Quantification is not possible via EDX since electron absorption and X-ray emission of the heavy elements (La, Gd) are too different from the light elements (C, H, N, S, O) for reliable comparison.

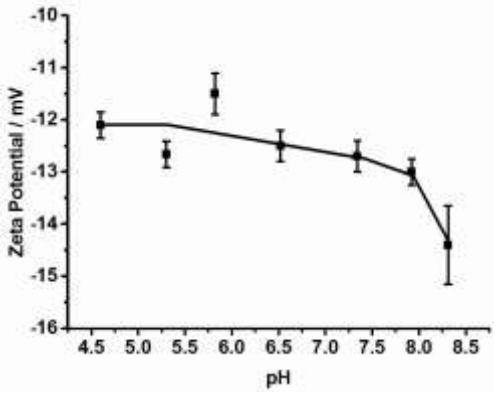

Fig. 3. Zeta potential of $M^{3+}[AMA]^{3-}$ (M = La, Gd) hybrid nanoparticles in water.

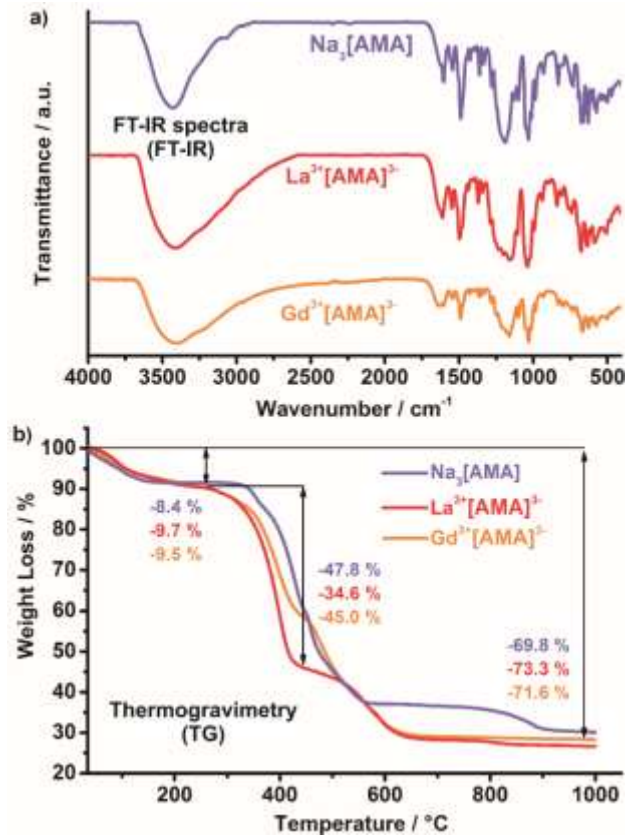

Fig. 4. Composition of the as-prepared $M^{3+}[AMA]^{3-}$ (M = La, Gd) hybrid nanoparticles with $Na_3[AMA]$ as a reference: a) FT-IR spectra; b) TG.

In view of the charge of the M^{3+} (M: La, Gd) and $[AMA]^{3-}$ ions, electroneutrality suggests a cation-to-anion ratio of 1 : 1. However, OH^- and/or H_2O have to be considered as eventual

Cite this: DOI: 10.1039/c0xx00000x

www.rsc.org/xxxxxx

PAPER

additional constituents. To reliably verify the cation-to-anion ratio and the chemical composition in $M^{3+}[AMA]^{3-}$, thermogravimetry (TG) was performed in order to prove the weight of the anion via thermal combustion as well as the presence of the cation via the weight of the thermal remnant. Prior to TG, the as-prepared nanoparticles were dried *in vacuum* at room temperature for 8 hours to remove all adsorbed solvents and water. Thereafter, TG shows an overall weight loss of 73% for $La^{3+}[AMA]^{3-}$ and 72% for $Gd^{3+}[AMA]^{3-}$ in a temperature range of 30 to 1000 °C (Figure 4b). These values correspond well to the calculated weight loss of 69% for the assumed composition $M^{3+}[AMA]^{3-}$ (*M*: La, Gd). The thermal remnant of the TG analysis was identified via X-ray powder diffraction as $La_2O_2(SO_4)$ and $Gd_2O_2(SO_4)$, respectively, and can be rationalized based on the following reaction:

$$2M^{3+}[C_{20}H_{11}N_2O_{10}S_3]^{3-} + 53½O_2 \rightarrow M_2O_2(SO_4) + 40CO_2 + 11H_2O + 2N_2 + 5SO_2 \text{ (with } M\text{: La, Gd)}$$

In sum, TG analysis confirms the expected composition $M^{3+}[AMA]^{3-}$ (*M*: La, Gd). To probe these results with an independent analytical tool, elemental analysis (EA) was performed and results in: C: 31.9 wt-%, N: 3.7 wt-%, and S: 11.6 wt-%. Within the experimental error, these experimental data are well in accordance with the calculated values: C: 35.6 wt-%, N: 4.1 wt-%, and S: 14.0 wt-%. All these data (FT-IR, EDX, TG, EA) substantiate the chemical composition $M^{3+}[AMA]^{3-}$ (*M*: La, Gd) of the inorganic-organic hybrid nanoparticles. Furthermore, it is to be noted that the nanoparticles are non-crystalline. Thus, X-ray powder diffraction analysis did not show any specific Bragg peak.

3.3 Fluorescence and magnetism of $M^{3+}[AMA]^{3-}$ inorganic-organic hybrid nanoparticles

As the inorganic-organic hybrid nanoparticles $M^{3+}[AMA]^{3-}$ (*M*: La, Gd) are of potential interest as contrast agents for multimodal imaging[2] or as magneto-optical marker in polymers,[1] we have next studied the optical and magnetic properties. Photographs illustrate the intense red emission of aqueous $M^{3+}[AMA]^{3-}$ suspensions upon excitation with a blue-light LED (λ_{max} = 465 nm) or green light (glass fiber with green filter, λ_{max} = 555 nm) (Figure 5a,b). Fluorescence spectroscopy quantifies the luminescence properties with excitation spectra of $M^{3+}[AMA]^{3-}$ showing an absorption in the 400 to 650 nm range (Figure 5c). Moreover, emission spectra validate intense red emission at λ_{max} = 700 nm (Figure 5c). Especially for *in vitro* and *in vivo* biomedical application (e.g. fluorescence microscopy),[2-5] such long-wavelength excitation is requested as it is less harmful to tissue (in contrast to UV light). Moreover, red and infrared emission is advantageous for optical imaging in terms of the autofluorescence of tissue and the penetration depth.[2-5]

A restriction of many organic fluorescent dyes and molecular optical markers (e.g. for fluorescence microscopy or signalling in polymers) is related to the phenomenon of photobleaching: thus, the photochemical destruction of the fluorescent organic dye under prolonged illumination with high-energy radiation (e.g. UV).[2-5] Highly photoresistant fluorescent dyes (e.g. perylene derivatives), on the other hand, are chemically resistant, and therefore, hardly metabolized after use which can restrict their biocompatibility.[23] Alternatively, various fluorescent dyes have been encapsulated in certain matrix materials. Here, nanocomposites with a fluorescent organic dye molecule (e.g. Cy3, Cy5, tetramethylrhodamine isothiocyanate/TRITC, fluorescein isothiocyanate/FITC, indocyanine green/ICG) encapsulated in an inorganic matrix material (e.g. SiO_2, $Ca_3(PO_4)_2$) are widely investigated. However, these materials show considerable photobleaching under UV illumination (Table 1).[7-13] On a timescale of some minutes to <1 hour of continuous illumination the fluorescence intensity is partly decreased by 50%. In many publications, photostability and photobleaching of the fluorescent nanoparticles were not even addressed. As photobleaching of the fluorescent organic dye proceeds on a short time scale, it severely restricts application in optical imaging and fluorescent thin-films. Generally, photobleaching of organic compounds is caused by reactive oxygen species (ROS) that are formed upon UV absorption and that lead to a cleavage of C–C/C–H bonds – thereby destroying the organic molecules.[24] Photobleaching is also a major drawback in comparison to fully inorganic fluorescence nanoparticles such as the quantum dots.[6]

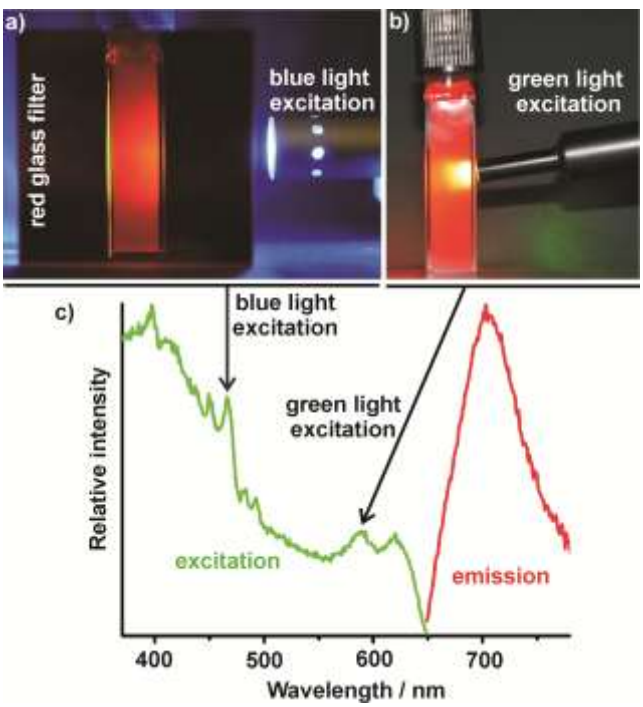

Fig. 5. Fluorescence of $M^{3+}[AMA]^{3-}$ (*M* = La, Gd) hybrid nanoparticles in water: a) Suspension excited via blue-light LED (λ_{max} = 465 nm); b) Suspension excited via green light (glass fiber with green filter, λ_{max} = 555 nm); c) Excitation and emission spectra.

To probe the photostability of the $M^{3+}[AMA]^{3-}$ hybrid nanoparticles, we have irradiated an aqueous suspension 15 hours with UV-light at λ_{max} = 310 nm (Figure 6a). For comparison, an aqueous solution of dissolved amaranth-red molecules (i.e. $Na_3[AMA]$) was irradiated under similar conditions (Figure 6a). Whereas the the dye solution shows the expected photobleaching with only 27% of the pristine emission intensity remaining after 15 hours of irradiation, the $M^{3+}[AMA]^{3-}$ suspension remains at constant emission intensity, and thus, does not show any significant photobleaching.

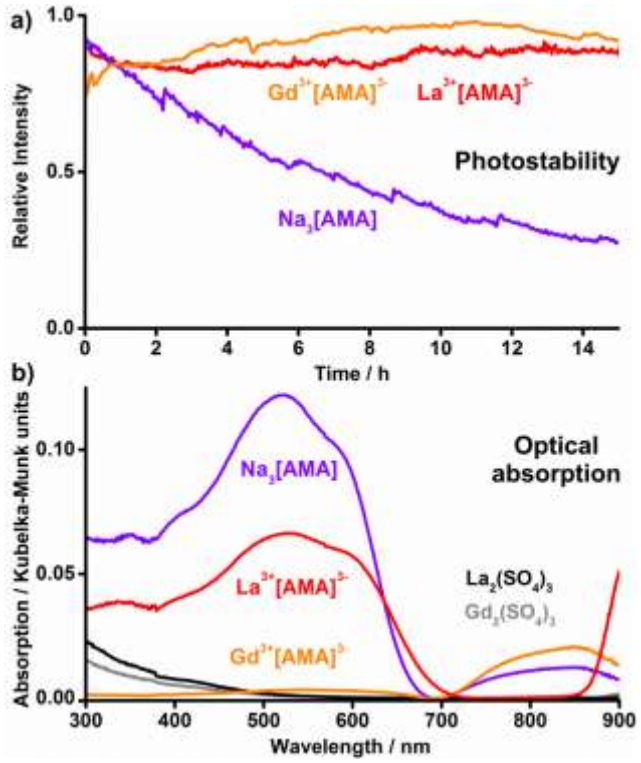

Fig. 6. Photostability of $M^{3+}[AMA]^{3-}$ (M = La, Gd) hybrid nanoparticles: a) UV-irradiation of aqueous suspensions (λ_{max} = 310 nm, 15 hours) in comparison to dissolved amaranth-red molecules (all in water); b) Absorption spectra in comparison to $Na_3[AMA]$, bulk-$La_2(SO_4)_2$, and bulk-$Gd_2(SO_4)_2$ (solid compounds mixed with $BaSO_4$ as standard white; the nanoparticles and the starting material $Na_3[AMA]$ were used with the same molar concentration of 33 mmol amaranth red).

As the remarkable photostability of $M^{3+}[AMA]^{3-}$ hybrid nanoparticles is a surprise and a major difference to other nanosystems with fluorescent organic dyes encapsulated in inorganic or polymer matrices (Table 1), we intended to elucidate the origin of the observed effect. To this concern, UV-Vis spectra of $M^{3+}[AMA]^{3-}$ hybrid nanoparticles were measured and compared based on the Kubleka-Munk formalism to the starting material $Na_3[AMA]$ as well as to bulk-$M_2(SO_4)_3$ (M = La, Gd) as references (Figure 6b). Here, the high reflectivity of the $M^{3+}[AMA]^{3-}$ hybrid nanoparticles is indicative in comparison to the $Na_3[AMA]$ reference. Especially, the high reflectivity of UV-light (<450 nm) can be called to account for the high photostability of the nanoparticles. At longer wavelength (450-700 nm), the nanoparticles show the characteristic absorption of the amaranth red dye that is needed for excitation. Altogether, the nanoparticles seem to exhibit a kind of intrinsic UV-protection due to their high reflectivity. Such high reflectivity is known for many sulphates, including $La_2(SO_4)_3$, $Gd_2(SO_4)_3$ (Figure 6b), or $BaSO_4$ – the latter is being widely used as standard white in optical spectroscopy.[25] Due to the high UV reflectivity, ROS formation at the particle surface can be assumed as low and does not destroy the fluorescent dye. Alternative inorganic materials such as SiO_2 or $Ca_3(PO_4)$, in contrast, are much less UV-reflective, and thus, show a limited stability of encapsulated fluorescent dye (Table 1). The different radii of Gd^{3+} and La^{3+} as well as the interaction of paramagnetic Gd^{3+} with near-surface OH radicals may have additional effects on reflectivity and photostability. Based on its remarkable photostability, $M^{3+}[AMA]^{3-}$ hybrid nanoparticles can be promising new fluorescent markers for optical imaging as well as for emissive polymers.

Tab. 1. Photobleaching of typical nanocomposites with fluorescent organic dyes encapsulated in inorganic or polymer matrix materials.

Encapsulated Fluorescent dye	Matrix material	Time of UV irradiation	Intensity after irradiation	Half-lifetime of emission	Ref.
Cy3	$Ca_3(PO_4)_2$	300 s	97%	Not measured	[9c]
Cy3	SiO_2	7 h	98%	Not measured	[12]
Cy5	SiO_2	200 s	25%	60 s	[9d]
Tetramethylrhodamine isothiocyanate/TRITC	SiO_2	2000 s	88%	Not measured	[8a]
Fluorescein isothiocyanate/FITC	SiO_2	30 min	70%	Not measured	[9e]
Indocyanine green/ICG	$Ca_3(PO_4)_2$	633 s	50%	633 s	[9f]
Indocyanine green/ICG	PLGA**	60 min	52%	60 min	[10a]
Nile red	PVK**	55 min	87%	Not measured	[13]
$M^{3+}[AMA]^{3-}$ (M = La, Gd)	Hybrid (no matrix)	15 h	100%	*infinite**	This work

*Since no photobleaching and decrease of intensity was observed for $M^{3+}[AMA]^{3-}$ hybrid nanoparticles (M = La, Gd) on a timescale of 15 hours, the formal half-lifetime of emission is infinite.
**PLGA: poly(lactic-co-glycolic acid); PFK: poly-N-vinylcarbazole.

In the case of the $Gd^{3+}[AMA]^{3-}$ hybrid nanoparticles, paramagnetism of seven unpaired electrons on Gd^{3+} is expected and can be interesting for magnetic resonance tomography (MRT) in medicine[26] as well as for magnetic detection and marking in polymer thin films.[1] Indeed, the as-prepared $Gd^{3+}[AMA]^{3-}$ nanoparticles already qualitatively show magnetic behaviour and can be attracted by a bar magnet (Figure 7a). This behaviour is quantified by magnetic measurements. Thus, $Gd^{3+}[AMA]^{3-}$ nanoparticles show a temperature dependence of the magnetic and the inverse magnetic susceptibility, measured at 10 kOe (Figure 7b). In order to consider the diamagnetic contribution of the amaranth red dye, the sum of Pascal's constants has been calculated and resulted in a diamagnetic contribution of -277×10^{-6} emu/mol.[27] Based on the linear temperature dependency of the inverse magnetic susceptibility in the whole temperature range from 3 to 350 K Curie paramagnetism can be clearly identified. A fit of the χ^{-1} data in the investigated temperature range using the Curie-Weiss law, revealed an effective magnetic moment of μ_{eff} = 6.83(1) μ_B per Gd atom and a Weiss constant of θ_p = 4.3(5) K. The effective magnetic moment is significantly smaller than the theoretical value of 7.94 μ_B for free Gd^{3+} ions. This is most likely due to residual water molecules in the nanoparticles that do not coordinate to the Gd^{3+} ions. As expected, no magnetic ordering for Gd^{3+} is observed from the *ZFC* data down to 3 K. The magnetization isotherms, measured at 70 and 300 K, finally,

Cite this: DOI: 10.1039/c0xx00000x

www.rsc.org/xxxxxx

PAPER

show a linear increase confirming the paramagnetic character (Figure 7c). No saturation effects are observed for higher magnetic fields, so that the magnetic moment at 70 K and 80 kOe is 1.2(1) μ_B / Gd atom, which is below the saturation magnetization of 7 μ_B according to $g_J \times J$.

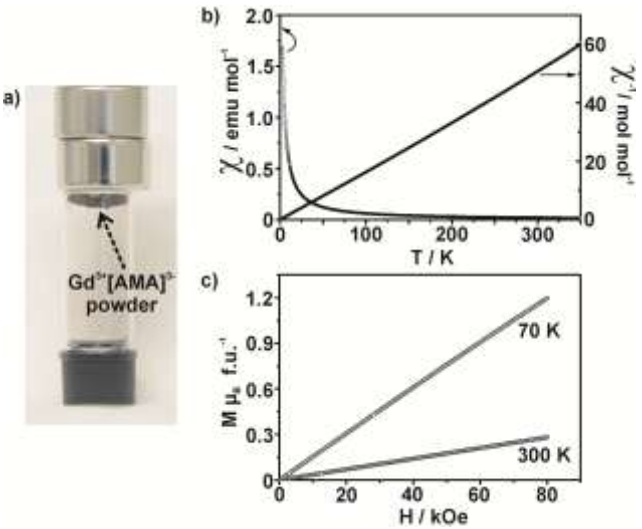

Fig. 7. Magnetic properties of $Gd^{3+}[AMA]^{3-}$ hybrid nanoparticles: a) Powder sample upside down with bar magnet attracting the nanoparticles; b) Susceptibility χ and its reciprocal χ^{-1} and its temperature dependance (at 10 kOe magnetic field strength); c) Magnetization at 70 K and 300 K depending on the external magnetic field.

In sum, the paramagnetic properties of the as-prepared $Gd^{3+}[AMA]^{3-}$ nanoparticles are very comparable to Gd^{3+}-containing compounds like Gd-DPTA (DPTA = diethylene-etriaminepentacetate) or Gd-DOTA (DOTA = 1,4,7,10-tetraazacyclododecane-N,N´,N´´,N´´´-tetraacetic acid) and their derivates that are commonly used as MRI contrast agents for more than 20 years.[28] Such Gd^{3+}-containing contrast agents drastically improve the quality of MR images by enhancing the relaxation rates of protons in body fluids and biological tissue.[29] For MRI, Gd-DOTA and Gd-DTPA are typically applied with about 0.1 mmol Gd^{3+} per kg of body weight.[30] In order to guarantee for similar Gd^{3+}-related magnetic spin concentration, the $Gd^{3+}[AMA]^{3-}$ nanoparticles need to be applied with about 0.1 mmol Gd^{3+} (~70 mg $Gd^{3+}[AMA]^{3-}$) per kg of body weight as well, which is a typical concentration range of nanoparticles.[31] Hence, the as-prepared $Gd^{3+}[AMA]^{3-}$ hybrid nanoparticles can become interesting contrast agent for MRI with the additional option of optical detection due to its fluorescence.

Besides materials characterization of the $M^{3+}[AMA]^{3-}$ (*M*: La, Gd) hybrid nanoparticles, we aimed at a first proof-of-the concept in view of the optical properties after encapsulation in polymer thin films and transfection into cells (Figures 8,9). Thus, $La^{3+}[AMA]^{3-}$ was redispersed in a mixture of ethylene glycol and citric acid that are thereafter thermally polymerized to polyester. Even comparably thick polyester films are fully transparent (Figure 8a). Although the nanoparticle concentration is low (0.2-5.0 mg $La^{3+}[AMA]^{3-}$ per mL of ethylene glycol), the polyester shows the red colour of the nanoparticles. The polyester film can be excited via a simple, low-cost blue-light LED (λ_{max} = 465 nm) and shows intense red light emission (Figure 8b, due to the higher refractive index of the polymer in comparison to air, light emission occurs especially at the polymer's front face).

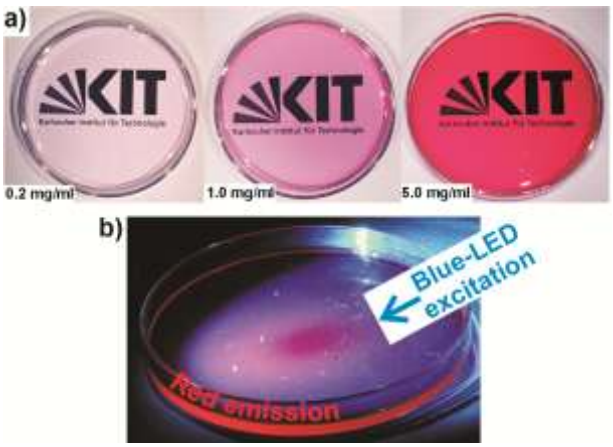

Fig. 8. $M^{3+}[AMA]^{3-}$ (*M* = La, Gd) hybrid nanoparticles in polymers: a) Photo of polyester films with $La^{3+}[AMA]^{3-}$ nanoparticles in different concentration (0.2-5.0 mg $M^{3+}[AMA]^{3-}$ per mL of ethylene glycol) in daylight; b) Photo of polyester film with $M^{3+}[AMA]^{3-}$ showing red emission upon excitation with a blue-light LED (λ_{max} = 465 nm).

Moreover, the $Gd^{3+}[AMA]^{3-}$ hybrid nanoparticles were co-incubated *in vitro* in a concentration of 50 µg in 1 mL of cell culture medium with murine alveolar macrophages of the MH-S cell line.[16] After 5 h incubation at 37 °C, a clear uptake of the nanoparticles by macrophages was demonstrated by fluorescence microscopy (Figure 9b). MH-S cells incubated with the nanoparticles at 4 °C, where the cellular metabolism and therefore internalization is strongly reduced, as well as MH-S cells cultivated without nanoparticles, do not show any comparable fluorescence (Figure 9a). $Gd^{3+}[AMA]^{3-}$ has only a low effect on the viability of MH-S cells (Figure 9c). In comparison to the untreated cells (100% viability), high concentrations of $Gd^{3+}[AMA]^{3-}$, e.g. 200 µg/mL, reduce the cell viability only by 30-35%, which could be partly due to the reduced concentration of culture medium (80 µL of medium + 20 µL of $Gd^{3+}[AMA]^{3-}$ suspension). Cells incubated with concentrations up to 100 µg/mL of $Gd^{3+}[AMA]^{3-}$ show more than 95% viability even after 48 h incubation (Figure 9c). In fact, a good biocompatibility is to be expected since both constituents Gd^{3+} and $[AMA]^{3-}$ are clinically approved and known for low toxicity.[14,28-30] Far red emission (>700 nm) as observed for $M^{3+}[AMA]^{3-}$ (*M*: La, Gd) or infrared emission, in fact, are most interesting for biomedical applications, in particular, optical imaging approaches in biological samples or *in vivo* as the light absorption by water and haemoglobin is minimal in this spectral range, resulting in optimal tissue penetration.[32]

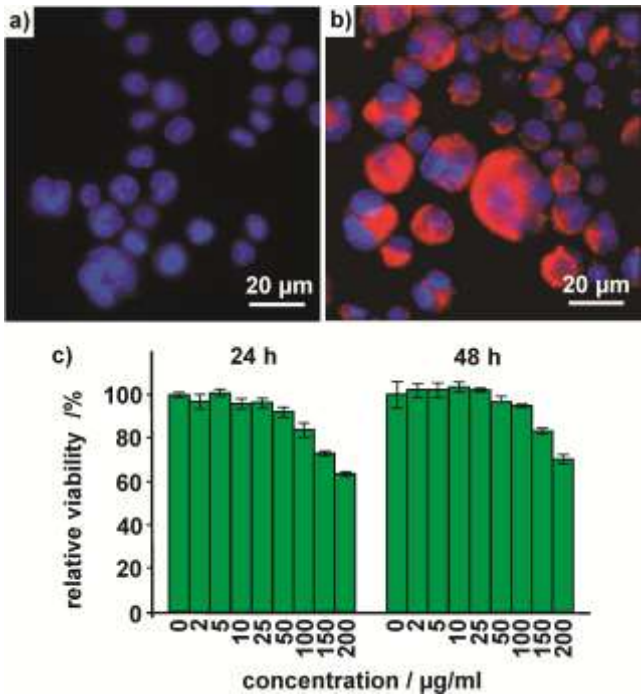

Fig. 9. $Gd^{3+}[AMA]^{3-}$ hybrid nanoparticles incubated with MHS macrophages: a) MHS cells cultivated without nanoparticles (cell nuclei show blue emission due to 4',6-diamidin-2-phenylindole/DAPI staining); b) Fluorescence microscopy showing $[Gd]^{3+}[AMA]^{3-}$ taken up by MHS cells (24 h after incubation with 50 µg/mL); c) Viability of MHS cells 24 hours and 48 hours after incubation with different concentrations of $Gd^{3+}[AMA]^{3-}$.

4. Conclusions and Outlook

$M^{3+}[AMA]^{3-}$ (M = La, Gd; AMA = amaranth red) nanoparticles are presented as a new class of sulfonate-based inorganic-organic hybrid materials. Herein, the fluorescent dye $[AMA]^{3-}$ – systematically named (4E)-3-oxo-4-[(4-sulfonatonaphth-1-yl)hydrazinyliden]naphthalin-2,7-disulfonate (as well named E123, C.I. 16185, Acid Red 27, C-Red 46, Echtrot D, or Food Red 9) – serves as the anion. Thus, the fluorescent dye is available in molar quantities and with an extraordinarily high load of 79 wt-%. $M^{3+}[AMA]^{3-}$ hybrid nanoparticles are prepared via aqueous synthesis. Colloidal suspensions in water are readily stable and exhibit a mean particle diameter of 47 nm. Particles size and chemical composition were studied with SEM, DLS, FT-IR, TG, EDX, and EA.

$M^{3+}[AMA]^{3-}$ shows intense red emission (λ_{max} = 700 nm) upon excitation at 400-650 nm and excellent photostability without any significant photobleaching after 15 hours of continuous UV irradiation (λ_{max} = 310 nm). The latter finding can be ascribed to the high reflectivity below 450 nm. Moreover, the $Gd^{3+}[AMA]^{3-}$ nanoparticles show the expected Gd^{3+}-related paramagnetism, comparable to conventional MRI contrast agents such as Gd-DOTA and Gd-DTPA. A first proof-of-the concept validates the red fluorescence of $M^{3+}[AMA]^{3-}$ hybrid nanoparticles in polyester films as well as the uptake and emission in MHS macrophages. Based on *i*) water-based synthesis, *ii*) biocompatible constituents, *iii*) extraordinary high dye load (79%), *iv*) low bleaching after 15 hours of continuous UV-irradiation, *v*) intense red emission and intrinsic Gd^{3+}-based magnetism, the here presented $M^{3+}[AMA]^{3-}$ (M = La, Gd) inorganic-organic hybrid nanoparticles can become very interesting as multimodal contrast agents in medicine and as magneto-optical markers in polymers. Next steps need to address live-time tests in polymers as well as the use of $M^{3+}[AMA]^{3-}$ hybrid nanoparticles in non-invasive optical imaging and MRI studies in mouse models of human diseases.

Acknowledgments

The authors are grateful to the Deutsche Forschungsgemeinschaft (DFG) for financial support. Furthermore, M.P. acknowledges the support of the DFG graduate School Karlsruhe School of Optics and Photonics (KSOP) at the KIT. J.N. and F.A. thank Bärbel Heidrich for excellent technical assistance in the cell experiments. O.N. is indebted to the NRW Forschungsschule *Molecules and Materials – A Common Design Principle* for PhD fellowship.

References

(1) H. Althues, J. Henle and S. Kaskel, *Chem. Soc. Rev.*, 2007, **36**, 1454 (Review).
(2) J. G. Fujimoto and D. Farkas, *Biomedical Optical Imaging*, Oxford University Press, Oxford, 2009.
(3) O. Chen, J. Zhao, V. P. Chauhan, J. Cui, C. Wong, D. K. Harris, H. Wei, H. Han, D. Fukumura and R. K. Jain, *Nature Mater.*, 2013, **12**, 445.
(4) I. Johnson (Ed.), *Molecular Probes Handbook: A Guide to Fluorescent Probes and Labelling Technologies*, Life Technologies Corporation, Darmstadt 2010.
(5) a) F. Persson, P. Bingen, T. Staudt, J. Engelhardt, J. O. Tegenfeldt and S. W. Hell, *Angew. Chem. Int. Ed.*, 2011, **50**, 5581. b) S.A. Hildebrand and R. Weissleder, *Curr. Opin. Chem. Biol*. 2010, **14**, 71. c) S. Luo, E. Zhang, Y. Su, T. Cheng and C. Shi, *Biomater.* 2011, **32**, 7127.
(6) a) X. Michalet, F. F. Pinaud, L. A. Bentolila, J. M. Tsay, S. Doose, J. J. Li, G. Sundaresan, A. M. Wu, S. S. Gambhir and S. Weiss, *Science* 2005, **307**, 538. b) Z. Liu, A. Kumbhar, D. Xu, J. Zhang, Z. Sun and J. Fang, *Angew. Chem.*, 2008, **120**, 3596. c) Z. Liu, A. Kumbhar, D. Xu, J. Zhang, Z. Sun and J. Fang, *Angew. Chem. Int. Ed.*, 2008, **47**, 3540. d) T. Jamieson, R. Bakhshi, D. Petrova, R. Pocock, M. Imani and A. M. Seifalian, *Biomater.*, 2007, **28**, 4717.
(7) a) I. Sokolov, S. Naik, *Small*, 2008, **4**, 934. b) T. Thomas, H. S. M. Morgan, E. I. Altinoglu, S. M. Rouse, A. Tabakovic, T. Tabouillot, T. J. Russin, S. S. Shanmugavelandy, P. J. Butler, P. C. Eklund, J. K. Yun, M. Kester and J. H. Adair, *Nano Lett.*, 2008, **8**, 4108.
(8) a) H. Ow, D. R. Larson, M. Srivastava, B. A. Baird, W. W. Webb and U. Wiesner, *Nano Lett.*, 2005, **5**, 113. b) X. Wu, M. Wu and J. X. Zhao, *Nanomed.*, 2013, **10**, 297. c) S. W. Ha, C. E. Camalier, G. R. Beck Jr. and J. K. Lee, *Chem. Commun*., 2009, **20**, 2881.
(9) a) D. Knopp, D. Tang and R. Niessner, *Anal. Chim. Acta*, 2009, **647**, 14. b) J. E. Fuller, G. T. Zugates, L. S. Ferreira, H. S. Ow, N. N. Nguyen, U. B. Wiesner and R. S. Langer, *Biomater.*, 2008, **29**, 1526. c) H. S. Muddana, T. T. Morgan, J. H. Adair and P. J. Butler, *Nano Lett*., 2009, **9**, 1559. d) A. A. Burns, J. Vider, H. Ow, E. Herz, O. Penate-Medina, M. Baumgart, S. M. Larson, U. Wiesner and M. Bradbury, *Nano Lett.*, 2008, **9**, 442. e) N. Zhang, E. Ding, X. Feng, Y. Xu, and H. Cai, *Colloids Surf. B Biointerfaces*, 2012, **89**, 133. f) E. I. Altınoğlu, T. J. Russin, J. M. Kaiser, B. M. Barth, P. C. Eklund, M. Kester and J. H. Adair, *ACS Nano*, 2008, **2**, 2075.
(10) a) C. Zheng, M. Zheng, P. Gong, D. Jia, P. Zhang, B. Shi, Z. Sheng, Y. Ma and L. Cai, *Biomater.*, 2012, **33**, 5603. b) G. A. Hughes, *Nanomed.*, 2005, **1**, 22.
(11) S. Parveen, R. Misra and S. K. Sahoo, *Nanomed*., 2012, **8**, 147.
(12) G. Chen, F. Song, X. Wang, S. Sun, J. Fan and X. Peng, *Dyes Pigm.*, 2012, **93**, 1532.
(13) S. Bhattacharyya, S. Prashanthi, P. R. Bangal and A. Patra, *J. Phys. Chem. C*, 2013, **117**, 26750.

Cite this: DOI: 10.1039/c0xx00000x

www.rsc.org/xxxxxx

PAPER

(14) a) European Food Safety Authority, *EFSA Journal*, 2010, **8**, 1649. b) COMMISSION REGULATION (EU) No 1129/2011 of 11 November 2011 amending Annex II to Regulation (EC) No 1333/2008 of the European Parliament and of the Council by establishing a Union list of food additives.
(15) R. Blume, H. Sommerfeld and H. Bader, *Naturwissenschaften im Unterricht Physik/Chemie*, 1989, **7**, 28.
(16) I. N. Mbawuike and H. B. Herscowitz, *J. Leukoc. Biol.*, 1989, **46**, 119.
(17) M. Roming, H. Lünsdorf, K. E. Dittmar and C. Feldmann, *Angew. Chem. Int. Ed.*, 2010, **49**, 632.
(18) E. Matijevic, *Chem. Mater.*, 1993, **5**, 412.
(19) V.K. LaMer and R. H. Dingar, *J. Am. Chem. Soc.*, 1950, **72**, 4847.
(20) R. Witter, M. Roming, C, Feldmann and A. S. Ulrich, *J. Colloid Interface Sci.*, 2013, **390**, 250.
(21) a) Y. Chao, P. P. Karmali, R. Mukthavaram, S. Kesari, V. L. Kouznetsova, I. F. Tsigelny and D. Simberg, *ACS Nano*, 2013, **7**, 4289. b) L. K. Bogart, A. Taylor, Y. Cesbron, P. Murray and R. Levy, *ACS Nano*, 2012, **6**, 5961.
(22) M. Snehalatha, C. Ravikumar, N. Sekar, V. S. Jayakumar and I. H. Joe, *Raman Spectros.*, 2008, **39**, 928.
(23) D. Görl, X. Zhang and F. Würthner, *Angew. Chem. Int. Ed.*, 2012, **51**, 6328.
(24) T. Tachikawa and T. Majima, *Chem. Soc. Rev.*, 2010, **39**, 4802 (Review).
(25) T. G. Germer, J. C. Zwinkels, B. K. Tsai, *Spectrophotometry: Accurate Measurement of Optical Properties of Materials*, Academic Press, Oxford 2014, p. 208.
(26) T.-H. Shin, Y. Choi, S. Kima and J. Cheon, *Chem. Soc. Rev.*, 2015, DOI: 10.1039/C4CS00345D.
(27) a) S.Y. Dan'kov, A. M. Tishin, V. K. Pecharsky and K. A. Gschneidner, *Phys. Rev. B*, 1998, **57**, 3478. b) G. A. Bain and J. F. Berry, *J. Chem. Educ.*, 2008, **85**, 532.
(28) W. J. Mulder, G. J. Strijkers, G. A. van Tilborg, A. W. Griffioen and K. Nicolay, *NMR Biomed.*, 2006, **19**, 142.
(29) S. Aime, M. Fasano, S. G. Crich and E. Terreno, *JBIC*, 1996, **1**, 312.
(30) a) E. J. Rummeny, E. Reimer and W. Heindel, Ganzkörper-MR-Tomographie, (Eds: Mödder, U.) Thieme, Stuttgart, New York, NY, 2011. b) C. A. Chang, L. C. Francesconi, M. F. Malley, K. Kumar, J. Z. Gougoutas, M. F. Tweedle, D. W. Lee and L. J. Wilson, *Inorg. Chem.* 1993, **32**, 3501.
(31) M. E. Davis, *MRS Bulletin*, 2012, **37**, 828.
(32) R. Weissleder, *Nature Biotechnol.*, 2001, **19**, 316.